Super-Klein tunneling of massive pseudospin-one particles

Y. Betancur-Ocampo, G. Cordourier-Maruri, V. Gupta, and R. de Coss
Departamento de Física Aplicada, Centro de Investigación y de Estudios Avanzados del IPN, A.P. 73 Cordemex 97310 Mérida, Yucatán, México

(Received 22 March 2017; revised manuscript received 28 June 2017; published 28 July 2017)

The transmission properties of massive particles with pseudospin-one through homogeneous and heterogeneous junctions are studied from an effective spin-orbit Hamiltonian. The addition of a mass term in the Hamiltonian creates an energy band gap with a flat band inside the gap. There are three possible scenarios for the location of the flat band: at the top of the valence band, at the bottom of the conduction band, and at the center of the energy band gap. We have studied how the position of the flat band affects the transmission through a general type of junction. We found that omnidirectional perfect transmission, called super-Klein tunneling, occurs even for massive particles with specific symmetrical conditions in the junction. In all other cases, an angular independent transmission is obtained, which can be considered as an attenuated super-Klein tunnelling. These effects emerge when the junction operates as a Veselago lens under the generalized focusing condition. Furthermore, we found that Klein tunneling is restored in the massless limit. The present findings may have important implications in the development of electronic devices based on quantum optics with massive pseudospin-one particles.

DOI: 10.1103/PhysRevB.96.024304

I. INTRODUCTION

The discovery of the extraordinary electronic and mechanical properties of graphene motivated the comprehensive study of two-dimensional Dirac materials [1–3]. One of the most amazing transmission phenomena in graphene is the Klein tunneling (KT), where perfect transmission through barrier potentials occurs due to the linear dispersion relation and pseudospin conservation of massless Dirac fermions [4–7]. KT and others pseudorelativistic phenomena are present in graphene as a result of its two-dimensional hexagonal lattice and the formation of Dirac cones in the electronic band structure [1,2]. Thus the issue about whether other physical systems presenting Dirac cones with higher dimensionality and pseudospin value, leading to novel and distinctive physics from those observed in two-dimensional pseudospin one-half Dirac materials, has been recently explored [8–22].

In the context of solid state systems, there are several structures such as two-dimensional τ_3 or Dice [15,16], Breathing [17], and Lieb lattices [18] whose band structure present Dirac cones. These systems have attracted a lot of attention because they can be described by the use of an enlarged pseudospin $S = 1$. In a similar way as in graphene, the dynamics can be depicted by a Dirac-like Hamiltonian with the particularity that, for certain energy conditions, they present an angular independent Klein tunneling through rectangular electrostatic barriers called super-Klein tunneling (SKT) [16,19,20]. When the conditions for SKT are fulfilled, an extraordinary Snell law allows all the refracted particle beams to be focused at one point, such as occurs in a Veselago lens [23–25]. That focusing particle flow could be useful for different applications and the design of devices based on electron quantum optics.

Systems with pseudospin-one involve, further the Dirac cones, a flat band in the middle of the dispersive bands. This flat band has important and unusual effects on the electronic properties due to its dispersionless nature. Particles from the flat band are attached to have an infinity effective mass being ideal for the realization of localized states [26–28]. Moreover, the flat band promises to be a key point for the search of room-temperature superconductivity [29,30]. It is important to mention that there are concrete examples of physical implementations such as ultracold atoms in optical lattice [14,20] and photonic crystals [19], where the physics of pseudospin-one particles can be simulated. Recently, a photonic Lieb lattice has served as a platform for the first experimental realization of localized compact states [27,28]. In condensed matter systems, the Lieb lattice has also been recently implemented [31,32]. A proposed material for the realization of a pseudospin-one Hamiltonian was put forward for strained blue phosphorene oxide [33].

Nevertheless, for the use of those physical systems in practical applications like electronics, the creation of a band gap is necessary. Furthermore, the presence of a band gap can also help to create quantum dots useful for implementing quantum information devices [34,35]. Therefore, the necessary modification of the Dirac cones to induce a topological phase transition can be represented by the addition of a mass term in the Dirac-like Hamiltonian. Thus, in the present work we theoretically study the effects of a flat band inside the band gap generated by the addition of a mass term on the transmission properties of the pseudospin-one particle. Here, the flat band location plays a crucial role. We focus our attention on how the SKT emerges and under what conditions this phenomena is preserved.

The paper is organized as follows. In the second section we describe our model, including three different ways to express a mass term in the systems. In the third section we analyze the reflection and transmission rate when the particle crosses through a general type of junction, which is modeled as a step potential. Using a general developed formulation, first we present results for the particle transmission when the mass term is the same in both sides or through a homogeneous junction. Then we analyze the cases when the mass term is different in each side of the junction, building a heterogeneous junction. In order to clarify the effect of the flat band in the transmission rate through the junction, in the fourth section, we show an analysis of the particle transmission from the flat band.

 ©2017 American Physical Society

Finally, in the fifth section we present our conclusions and final remarks.

II. MODEL

To describe the band structure of pseudospin-one Dirac systems near to the high symmetry K point of the first Brillouin zone in a Dice lattice [15,16] or near to the Γ point in a Lieb lattice [20], we employ an effective Dirac-like model which is useful to study the dynamics of massive pseudospin-one particles around those points. Such a model considers a spin-orbit Hamiltonian written as

$$H = v_F \boldsymbol{S}\cdot\boldsymbol{p} + \Delta M, \tag{1}$$

where v_F is the Fermi velocity, $\boldsymbol{p} = -i\hbar\nabla$ is the linear momentum operator, $\boldsymbol{S} = S_x\hat{x} + S_y\hat{y}$ is the spin operator in terms of the spin-one matrices

$$S_x = \frac{1}{\sqrt{2}}\begin{pmatrix}0&1&0\\1&0&1\\0&1&0\end{pmatrix}, \quad S_y = \frac{1}{\sqrt{2}}\begin{pmatrix}0&-i&0\\i&0&-i\\0&i&0\end{pmatrix}, \tag{2}$$

and the product ΔM can be considered as a mass generation term in the Hamiltonian, because it induces a gap opening with an effective mass defined as $m = \Delta/v_F^2$. This effective Hamiltonian (1) is frequently found expanding the tight-binding (TB) Hamiltonian to nearest neighbors of a Dice lattice around the K point of the first Brillouin zone [15,16], where the mass term can be constructed using different on-site energies. For instance, the U term is obtained from the on-site energies for the A or B sublattice in the τ_3 model and the Lieb lattice. Otherwise, Hamiltonian (1) can also be derived expanding the TB Hamiltonian of ultracold atoms in an optical Lieb lattice around the Γ point of the first Brillouin zone and the mass term appears tuning the laser intensities [20]. In this work, we study three special cases for M having the form

$$M = S_z = \begin{pmatrix}1&0&0\\0&0&0\\0&0&-1\end{pmatrix}, \quad M = \pm U = \pm\begin{pmatrix}1&0&0\\0&-1&0\\0&0&1\end{pmatrix}. \tag{3}$$

The case where $M = S_z$ has been used to describe the effect of applied magnetic field on bosonic band structure in $SrCu_2(BO_3)_2$ [21]. This case can also be seen as an extension of the usual mass term in graphene [36]. The solution of the secular problem with $M = S_z$ in (1) leads to the following dispersion relations:

$$E_0 = 0, \quad E_s = s\sqrt{\Delta^2 + v_F^2 p^2}, \tag{4}$$

where $s = 1$ (-1) corresponds to the conduction (valence) band. We note that the dispersionless flat band is located at zero energy, whereas the valence and conduction bands are separated by a gap of magnitude 2Δ, as shown in Fig. 1(a). The corresponding wave functions can be expressed as

$$|\Psi_0\rangle = \frac{1}{\sqrt{2}}\begin{pmatrix}\beta\, e^{-i\phi}\\ -\sqrt{2}\frac{\Delta}{E}\\ -\beta\, e^{i\phi}\end{pmatrix}, \quad |\Psi_s\rangle = \frac{1}{2}\begin{pmatrix}\alpha\, e^{-i\phi}\\ \sqrt{2}s\beta\\ \gamma\, e^{i\phi}\end{pmatrix}, \tag{5}$$

where $\alpha = 1 + (s\Delta/E)$, $\beta = \sqrt{1-(\Delta/E)^2}$, $\gamma = 1 - (s\Delta/E)$, and $E = \sqrt{\Delta^2 + v_F^2 p^2}$ is the particle energy. The wave function's phase ϕ is related with the propagation direction as $\tan(\phi) = p_y/p_x$, with p_x and p_y the components of the momentum vector $\boldsymbol{p}$.

On the other hand, the cases with $M = \pm U$ were used to describe the site energy on different sublattices in a Lieb superlattice [37]. That case can also be found in photonic crystals [38] and ultracold atoms in optical lattices [20]. Thus, solving the secular problem with $M = \pm U$ in (1), it is found that the energies have the form

$$E_0 = \pm\Delta, \quad E_s = s\sqrt{\Delta^2 + v_F^2 p^2}. \tag{6}$$

In this case, the flat band is located at the bottom of the conduction band for $M = U$ and at the top of the valence band for $M = -U$, as seen in Figs. 1(b) and 1(c). The respective wave functions for $M = U$ are given by

$$|\Psi_0\rangle = \frac{1}{\sqrt{2}}\begin{pmatrix}e^{-i\phi}\\ 0\\ -e^{i\phi}\end{pmatrix}, \quad |\Psi_s\rangle = \frac{1}{2}\begin{pmatrix}\sqrt{\alpha}e^{-i\phi}\\ s\sqrt{2\gamma}\\ \sqrt{\alpha}e^{i\phi}\end{pmatrix}. \tag{7}$$

Wave functions for the case $M = -U$ are obtained with the substitutions $\alpha \to \gamma$ and $\gamma \to \alpha$ in (7). Although the three expressions of M open a band gap of the same magnitude

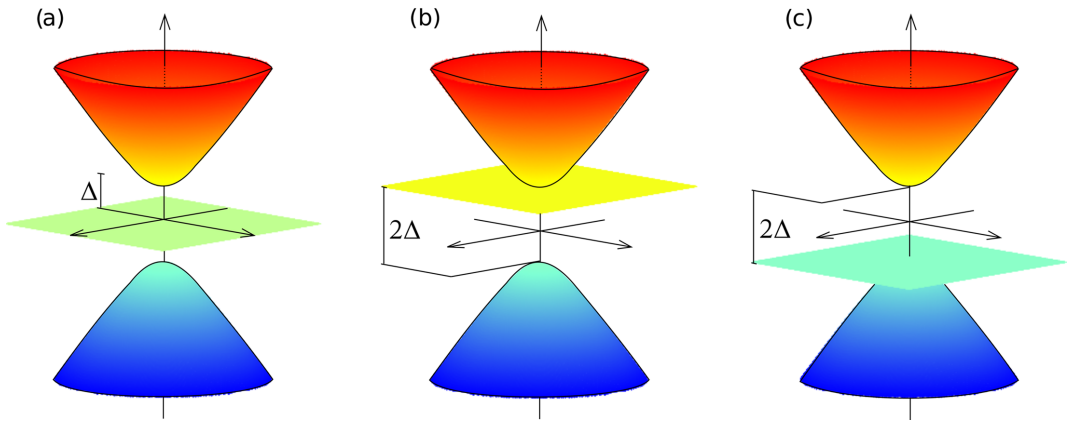

FIG. 1. Graphical representation of the dispersion relations of the Hamiltonian (1). (a) For the case of mass generation term $M = S_z$, while (b) and (c) correspond to the cases $M = U$ and $M = -U$, respectively.

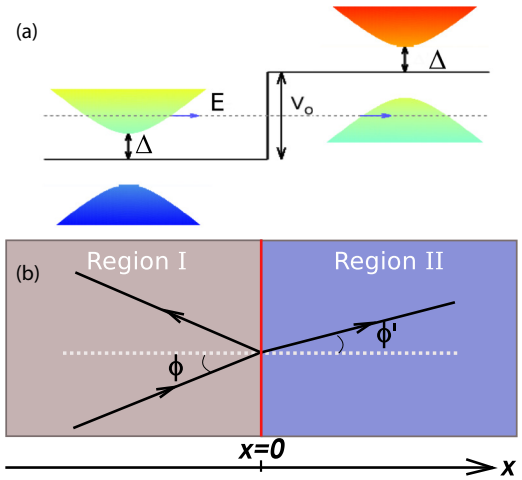

FIG. 2. (a) Scheme of a junction depicted by a step potential V_0 and the corresponding energy band structure. (b) Description of the particle scattering through the junction; a particle beam is injected from the left in region I, with an incidence angle ϕ. Then, a reflected beam comes back in region I, while a refracted beam is transmitted through region II with a refraction angle ϕ'.

2Δ, the wave functions (5) and (7) display different forms. Consequently, the specific location of the flat band must have strong consequences on the transmission probability through a junction.

III. TRANSMISSION THROUGH A JUNCTION

We analyze the particle transmission through a homogeneous and heterogeneous junction, which can be depicted by a step potential of high V_0, for the three cases of M described above. A device, as shown in Fig. 2(a), can be conformed by a material whose excitations are described through the Dirac equation of pseudospin-one particles. Thus triplons in $SrCu_2(BO_3)_2$ in the presence of a weak magnetic field represent a feasible option [21]. Usually, a homogenous junction is obtained with two external gates at regions I and II, and it is considered abrupt when the condition $k_F d < 1$ is satisfied, with k_F being the magnitude of the Fermi wave vector and d the split-gate length. Under this assumption, we avoid the angular filter of particle beams beyond the normal incidence [39–42]. It is important to note that the coherence length and the mean free path of the particle are expected to be larger than the device's dimensions, allowing the system to be within the ballistic transport regime. Other systems can be proposed using electromagnetic waves in photonic crystals, where the junction is simulated shrinking the distance among dielectrics [19].

In the device shown in Fig. 2(b), a point source injects the ballistic particles with a wide angular distribution. The junction located at $x = 0$ scatters the incident particle flow producing a reflected beam that comes back along the $-\phi$ direction; meanwhile, a refracted beam crosses the interface, where an extended drain collects the output beam in the region II. In general, the dynamics of this system is depicted by the effective Hamiltonian

$$H = v_F \boldsymbol{S}\cdot\boldsymbol{p} + Q(x), \quad Q(x) = \begin{cases} \Delta M, & \text{if} \quad x < 0, \\ \Delta' M' + V_0, & \text{if} \quad x \geqslant 0, \end{cases} \tag{8}$$

where the effect of V_0 on the band structure is to raise the Dirac cone energy by V_0 in the $x \geqslant 0$ region, as seen in Figs. 2(a), 3(a), 5(a), and 5(c). We consider the case when $\Delta M = \Delta' M'$ as a homogeneous junction where the only difference in the regions forming the sides of the junction is the potential. In order to clarify the role of the flat band in the particle transmission, we also analyze the case when $\Delta M \neq \Delta' M'$. These kind of junctions can be considered as heterogeneous. A more sophisticated device must be designed to implement a heterogeneous junction because the regions I and II have to be conformed by structures with different flat band position. For instance, the region I can be constituted by a photonic Lieb lattice having geometrical parameters different to the lattice in the region II.

Because the flat band position depends on the election of the mass term, we could locate the flat bands in a total of nine possible configurations in a junction: three possible positions for the flat band, at the top of the valence band, at the bottom of the conduction band, or in the middle of the band gap, in each region. Three of these nine configurations correspond to homogeneous junctions and all others to heterogeneous junctions, if $\Delta = \Delta'$. We denote each configuration with the label (i, j), where $i, j = -1$, 0, and 1. Thus the value of i (j) indicates the location of the flat band in the region I (region II). Hence, when the flat band is located at the bottom of the conduction band in both regions correspond to $i, j = 1$, and when the flat band is located at the top of the valence band in both regions correspond to $i, j = -1$, while the system when the flat band is located at the middle of the band gap in both regions is labeled as $i, j = 0$. For the (i, j) system, we express the wave function for states at the conduction or valence band in region I ($x < 0$) as

$$|\Psi_I\rangle = \frac{1}{2}\begin{pmatrix} a\,e^{-i\phi} \\ sb \\ c\,e^{i\phi} \end{pmatrix} e^{ip_x x/\hbar} + \frac{1}{2} r \begin{pmatrix} a\,e^{i\phi} \\ -sb \\ c\,e^{-i\phi} \end{pmatrix} e^{-ip_x x/\hbar}, \tag{9}$$

where ϕ is the incident angle and $p_x = |E|\cos(\phi)/v_F$ is the component of the linear momentum on the x direction. The coefficients a, b, and c can be determined from the wave functions (5) or (7). The coefficient r is the probability amplitude for the reflected beam. In region II, the transmitted wave function is given by

$$|\Psi_{II}\rangle = \frac{1}{2} t \begin{pmatrix} a' e^{-i\phi'} \\ s' b' \\ c' e^{i\phi'} \end{pmatrix} e^{ip'_x x/\hbar}. \tag{10}$$

The quantities with prime correspond to the region II and the a', b', and c' coefficients are defined in terms of $\alpha' = 1 + s'\Delta'/|E - V_0|$, $\beta' = \sqrt{1 - \Delta'^2/(E - V_0)^2}$, $\gamma' = 1 - s'\Delta'/|E - V_0|$, and $s' = \mathrm{sgn}(E - V_0)$, where they can be obtained from (5) or (7) by replacing the unprimed quantities a, b, and c by the quantities a', b', and c'. t is the amplitude for the transmitted beam, ϕ' is the refraction angle, and $p_x = |E - V_0|\cos(\phi')/v_F$ is the x component of

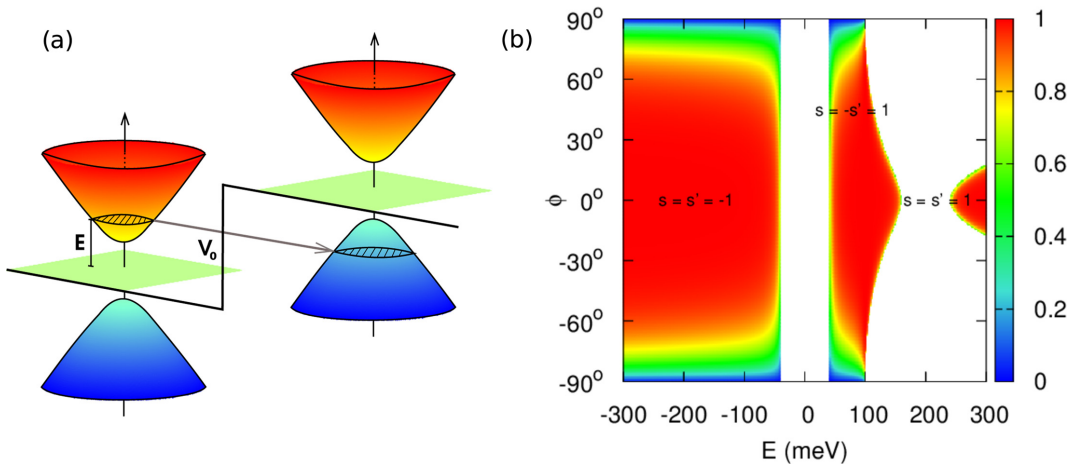

FIG. 3. System (0,0) with $M = S_z$ in both regions of the junction: (a) scheme of the band structure and (b) transmission probability as a function of the energy E and the incidence angle ϕ, using the set of values $\Delta = \Delta' = 40$ meV, $V_0 = 200$ meV, and the Fermi velocity $v_F = 0.83\times10^6$ ms^{-1}.

the momentum vector. We allow the use of different values of the half-gap energy in both sides of the step potential, Δ for the region I and Δ' for the region II. Thus, for a state defined as $|\Psi\rangle = (\psi_1(x),\psi_2(x),\psi_3(x))$ where $\psi_i(x)$ $(i = 1,2,3)$ are the components of the wave function $|\Psi\rangle$, the determination of the probability amplitudes r and t is performed using the boundary conditions at $x = 0$ from the wave functions (9) and (10). The boundary conditions are obtained integrating the Dirac equation from $-\epsilon$ to ϵ and then taking the limit $\epsilon \to 0$. Assuming that $M(x)$, $V(x)$, and $\psi_i(x)$ are all finite, we found that $\psi_2(0^-) = \psi_2'(0^+)$ and $\psi_1(0^-) + \psi_3(0^-) = \psi_1'(0^+) + \psi_3'(0^+)$ must be continuous. Solving the 2×2 linear equation system for r and t with these boundary conditions, the reflection probability $R = |r|^2$ has the form

$$R_{ij} = \frac{(s\xi_{ij}\cos\phi - s'\xi'_{ij}\cos\phi')^2 + (s\chi_{ij}\sin\phi - s'\chi'_{ij}\sin\phi')^2}{(s\xi_{ij}\cos\phi + s'\xi'_{ij}\cos\phi')^2 + (s\chi_{ij}\sin\phi - s'\chi'_{ij}\sin\phi')^2}, \tag{11}$$

TABLE I. Parameters defining the reflection probability according to Eq. (11), for each system configuration (i, j).

(i,j) system	$j=-1$	$j=0$	$j=1$
$i=-1$	$\xi_{-1-1} = \sqrt{\alpha'\gamma}$ $\xi'_{-1-1} = \sqrt{\alpha\gamma'}$ $\chi_{-1-1} = 0$ $\chi'_{-1-1} = 0$	$\xi_{-10} = \beta'\sqrt{\gamma}$ $\xi'_{-10} = \sqrt{\alpha}$ $\chi_{-10} = 0,$ $\chi'_{-10} = s'\frac{\Delta'}{\lvert E-V_0\rvert}\sqrt{\alpha}$	$\xi_{-11} = \sqrt{\gamma\gamma'}$ $\xi'_{-11} = \sqrt{\alpha\alpha'}$ $\chi_{-11} = 0$ $\chi'_{-11} = 0$
$i=0$	$\xi_{0-1} = \sqrt{\alpha'}$ $\xi'_{0-1} = \beta\sqrt{\gamma'}$ $\chi_{0-1} = s\frac{\Delta}{E}\sqrt{\alpha'}$ $\chi'_{0-1} = 0$	$\xi_{00} = \beta'$ $\xi'_{00} = \beta,$ $\chi_{00} = s\beta'\frac{\Delta}{E}$ $\chi'_{00} = s\beta\frac{\Delta}{E}$	$\xi_{01} = \sqrt{\gamma'}$ $\xi'_{01} = \beta\sqrt{\alpha'}$ $\chi_{01} = s\frac{\Delta}{E}\sqrt{\gamma'},$ $\chi'_{01} = 0$
$i=1$	$\xi_{1-1} = \sqrt{\alpha\alpha'}$ $\xi'_{1-1} = \sqrt{\gamma\gamma'}$ $\chi_{1-1} = 0,$ $\chi'_{1-1} = 0$	$\xi_{10} = \beta'\sqrt{\alpha}$ $\xi'_{10} = \sqrt{\gamma}$ $\chi_{10} = 0$ $\chi'_{10} = s'\frac{\Delta'}{\lvert E-V_0\rvert}\sqrt{\gamma}$	$\xi_{11} = \sqrt{\alpha\gamma'}$ $\xi'_{11} = \sqrt{\alpha'\gamma}$ $\chi_{11} = 0$ $\chi'_{11} = 0$

where the quantities ξ_{ij}, ξ'_{ij}, χ_{ij}, and χ'_{ij} depend on α, α', β, β', γ, and γ' according to the chosen configuration for the system among the nine options. The nine groups of coefficients for each case are specified in Table I.

The relation between ϕ and ϕ' is established from the corresponding Snell's law, which is obtained from the conservation of the momentum in the y direction (p_y) and E, leading to the following expression:

$$\sin\phi' = \frac{|E|\beta}{|E - V_0|\beta'}\sin\phi, \tag{12}$$

where negative refraction of massive pseudospin-one particles in interband transmissions is obtained in a similar way as in massless pseudospin-1/2 case. This is possible due to the inversion of $\boldsymbol{p}$ when the particle is transmitted from the conduction (valence) in region I, to the valence (conduction) band in region II. Thus one can design a device, such as the Veselago lens in graphene [25], which focuses the particle beams towards a point. This phenomena occurs for the specific energy $E_c = V_0/2$ with $|V_0| \geqslant 2\Delta$ where the transversal sections of the Dirac cones have the same radius. In a system with different masses $\Delta \neq \Delta'$ is possible to prove that a general focusing condition is given by

$$E_c = V_0/2 + (\Delta^2 - \Delta'^2)/2V_0, \tag{13}$$

where $V_0 \geqslant \Delta + \Delta'$. Then, the Snell's law (12) evaluated at this energy can be reduced to $\phi' = \pi - \phi$, which indicates the presence of a focused particle beam at the refraction region.

IV. TRANSMISSION THROUGH A HOMOGENEOUS JUNCTION

We start analyzing particle transmission for the case (i) $M = S_z$ which corresponds to the system (0,0), and later the cases (ii) $M = \pm U$ corresponding to the systems $(\pm1,\pm1)$.

(i) $M = S_z$: system (0,0).

Thereby, with the help of the general equation (11) and Table I, the reflection probability for the case (0,0)

$$R = \frac{\left(s\,\cos\phi - \frac{\beta}{\beta'}s'\cos\phi'\right)^2 + \left(\frac{\Delta}{|E|}\sin\phi - \frac{\beta\Delta}{\beta'|E'|}\sin\phi'\right)^2}{\left(s\,\cos\phi + \frac{\beta}{\beta'}s'\cos\phi'\right)^2 + \left(\frac{\Delta}{|E|}\sin\phi - \frac{\beta\Delta}{\beta'|E'|}\sin\phi'\right)^2} \tag{14}$$

is obtained. In order to evaluate the transmission probability of massive pseudospin-one particles with $M = S_z$, we use the expressions (12) and (14) where the transmission probability is $T = 1 - R$. Thus Fig. 3(b) shows the transmission probability T as a function of the incidence angle ϕ and energy E. The set of values used for the parameters involved in this calculation are $\Delta = \Delta' = 40$ meV, $V_0 = 200$ meV, and the Fermi velocity $v_F = 0.83\times10^6$ ms^{-1} was taken as in pristine graphene [2]. We note that there are two transmission gaps with a threshold of $2\Delta = 80$ meV, which induces three regimes in the transmission spectra. One of the main consequences of the band gap structure in the system is the separation between the intraband and interband transmissions. The first regime shows the transmission probability from the valence band in the region I to the valence band in the region II ($s = -1$, $s' = -1$). In this regime, the massive pseudospin-one particles behave as those massless pseudospin-1/2 and Klein tunneling for normal incidence is observed for $|E| \gg \Delta$. This result is well understood when we identify the resemblance with ultrarelativistic particles because the rest mass energy becomes negligible compared with the kinetic energy. In contrast, for $|E| \approx \Delta$ the Klein tunneling is completely lost. The second regime corresponds to the transmissions from the conduction band in region I to the valence band in region II ($s = 1$, $s' = -1$) and occurs when $V_0 > 2\Delta$. Here, as can be observed in Fig. 4(a), we found the formation of SKT at the energy $E = V_0/2 = 100$ meV, which is the same value predicted for massless pseudospin-one systems [16,19,20]. For this energy, the Snell's law (12) is simplified to $\phi' = \pi - \phi$ indicating that the refracted beam is met again in a symmetric spot within the region II. Further, in this regime we can see that there is a wide incidence region and energies where a high transmission rate is observed. This result contrasts with massive pseudospin-1/2 Dirac fermions in graphene, where perfect nonresonant tunneling never occurs for interband transmission [36]. Finally, the third regime consists of transmissions from the conduction band in region I to the conduction band in region II ($s = 1$ to $s' = 1$). Likewise that for the first regime, Klein tunneling is observed for high energies due to the massless limit.

(*ii*) $M = \pm U$: systems $(\pm1,\pm1)$.

Now we consider the case $M = U$ or system (1,1), whose results can be generalized with the substitutions $\alpha \to \gamma$ and $\gamma \to \alpha$ for the $M = -U$ case or system $(-1,-1)$. Using the general equation (11) and Table I, the reflection probability for the case (1,1) is given by

$$R = \left(\frac{s\,\cos\phi - s'\sqrt{\frac{\alpha'\gamma}{\alpha\gamma'}}\cos\phi'}{s\,\cos\phi + s'\sqrt{\frac{\alpha'\gamma}{\alpha\gamma'}}\cos\phi'}\right)^2. \tag{15}$$

The transmission probability for the cases $M = U$ and $M = -U$ as a function of the incidence angle ϕ and the energy E is plotted in Figs. 5(b) and 5(d), respectively. The values

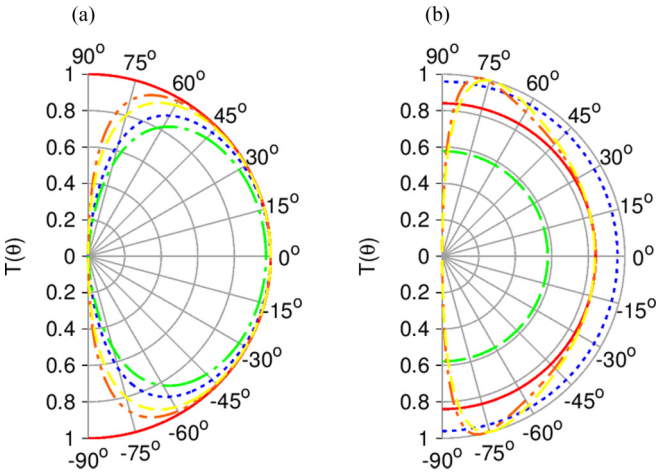

FIG. 4. (a) Transmission probability as a function of ϕ for the (0,0) system: SKT behavior (red curve) is obtained with the set of values $V_0 = 200$ meV, $E = V_0/2 = 100$ meV, and $\Delta = \Delta' = 40$ meV for equal masses in both sides of the junction. Orange (yellow) curve shows how SKT is lost when the value of energy is changed to $E = 95$ ($E = 90$) meV. Such an effect also is affected setting the masses to be different in both regions with $\Delta = 0$ ($\Delta = 90$) and $\Delta' = 40$ meV, as shown in blue (green) curve, where $E = 96$ ($E = 116$) meV is calculated from the general focusing condition (13). (b) Transmission probability as a function of ϕ for the (1,1) system using the same set of values as in (a): red, blue, and green curves show ASKT (see text).

of the parameters used in these plots are the same as those used in Fig. 3(b). As we can see from Figs. 3(b) and 5(b), the transmission probability show some similarities with the case $M = S_z$. First, the two transmission gaps are located at the same energy values because they only depend on the band gap energy. Likewise, the massless limit is obtained for high energy values and the Klein tunneling for normal incidence is restored for intraband transmission regimes ($s = -1$, $s' = -1$ and $s = 1$, $s' = 1$). However, in the interband transmission regime ($s = -1$, $s' = 1$) the SKT is absent. If we focus at the energy value of $E = V_0/2$, we found that the transmission probability is not perfect but it is omnidirectional as can be seen in Fig. 4(b). This reminiscence of the SKT can be considered as an attenuated super-Klein tunneling (ASKT). Furthermore, there are also some clear differences between transmission probabilities corresponding to U and $-U$ that become more evident near to the transmission gaps. Whereas in the U case, the transmission probability is higher for angles of incidence far from the normal incidence within the interband transmission, the $-U$ case shows a similar behavior within the intraband transmission regime for energies near to $E = -\Delta$. This is an unusual effect in massive pseudospin-one particles transmission because in the nonrelativistic regime the transmission probability is always less than one. Such distinctive features for the transmission of massive pseudospin-one particles make evident the drastic effect caused by the flat band location. Therefore, a natural issue to analyze emerges about whether the transmission probability presents important changes when the two regions forming the junction have different flat band location and masses.

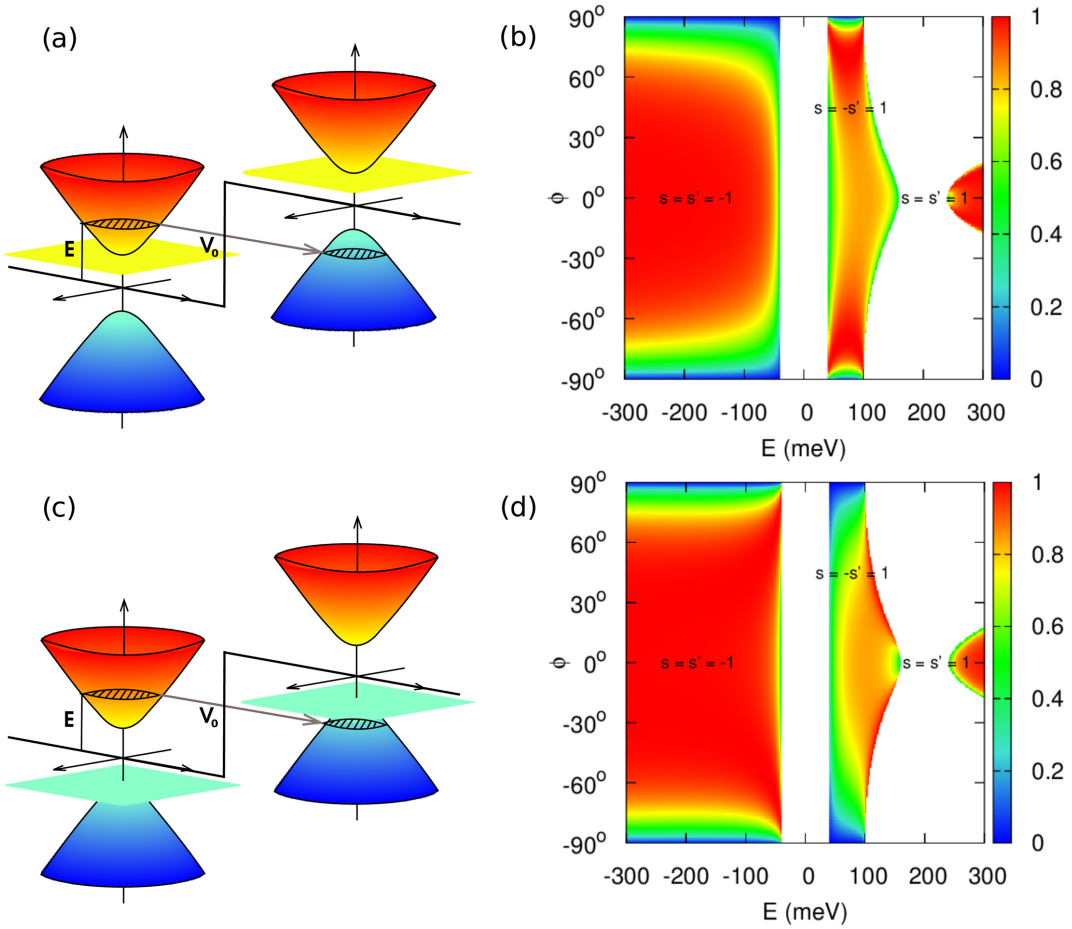

FIG. 5. Scheme of the band structure for the systems (a) $(1,1)$ and (c) $(-1,-1)$. Transmission probability as a function of the incidence angle ϕ and the energy E for the systems (b) $(1,1)$ and (d) $(-1,-1)$, using the set of values $\Delta = \Delta' = 40$ meV, $V_0 = 200$ meV, and the Fermi velocity value $v_F = 0.83\times10^6$ ms^{-1}.

V. TRANSMISSION THROUGH A HETEROGENEOUS JUNCTION

For the configurations (i,j) with $i \neq j$ a heterogeneous junction is created. The transmission probabilities for these cases can be obtained using the general equation (11), the parameter values shown in Table I, and the relation $T = 1 - R$. Figure 6 shows the transmission probabilities as a function of energy E and incidence angle ϕ for the systems $(1,-1)$ and $(-1,1)$. We set $\Delta = \Delta' = 40$ meV, $V_0 = 200$ meV as in the previously discussed cases (0,0), (1,1), and $(-1,-1)$,

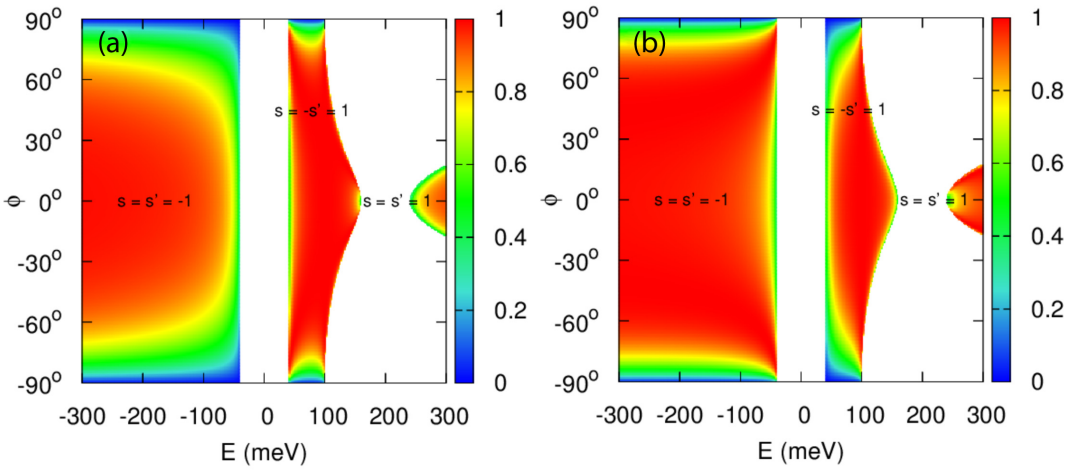

FIG. 6. Transmission probability as a function of the energy E and the incidence angle ϕ, for the systems (a) $(1,-1)$ and (b) $(-1,1)$, with the same set of parameter values as in Fig. 5.

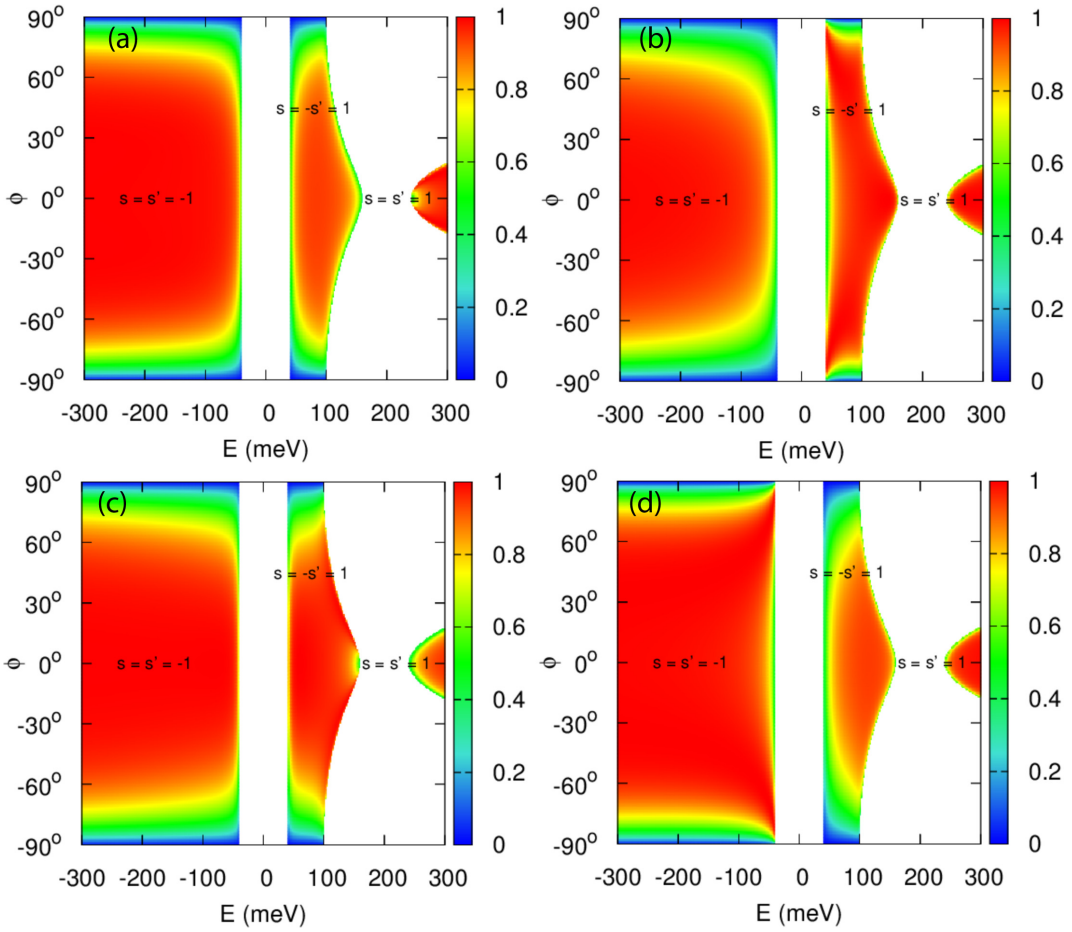

FIG. 7. Transmission probability as a function of the energy E and the incidence angle ϕ, for the systems (a) (0,1), (b) (1,0), (c) (0,−1), and (d) (−1,0).

and the Fermi velocity value of $v_F = 0.83\times10^6$ ms^{-1} is used. Then, we can note that SKT appears again at the focusing energy condition $E = V_0/2$. This result indicates that the asymmetrical location of the flat bands produces the same effect as that in the (0,0) system. From the reflection coefficient (11) and evaluating for $\phi' = \pi - \phi$, we can prove that $R_{-11} = R_{1-1} = R_{00} = 0$, which is independent of ϕ. Hence the predicted SKT for massless pseudospin-one particles [16,19,20] is also achieved with the mass generation term and depends on the flat band location. Furthermore, we note that the intraband transmission regime of (−1,1) for $E < -\Delta$ has a similar behavior than for the (−1, − 1) configuration, as shown in Fig. 5(d). This feature of the transmission probability presenting high values when $|\phi|$ is increased within the intraband transmission $s = s' = -1$ are typical in the $(-1, j)$ systems. In general for a (i, j) system with $V_0 \gg \Delta + \Delta'$, the intraband transmission $s = s' = -1$ ($s = s' = 1$) is mainly governed by the i (j) index, because the flat band in region II (I) is located far away from the energy range of the regime of interest.

Systems with the (0,1), (1,0), (0,−1), and (−1,0) configurations do not present SKT or ASKT, as seen in Fig. 7. In all the cases, when $E \gg \Delta$ or Δ', the transmission of massive particles is very similar to massless cases. Moreover, the Klein tunneling for normal incidence is still observed. The perfect transmission appears for a wide range of ϕ which is a distinctive feature of pseudospin-one particles. For energies near to the band gap energy, the mass and the location of the flat band begin to be relevant. It is important to note that for energies satisfying $|E_c| < E < |V_0| - \Delta'$ and $E > |V_0| + \Delta'$, transmission modes occur for the incidence range $-\phi_c \leqslant \phi \leqslant \phi_c$, where $\phi_c = \arcsin(|E - V_0|\beta'/E\beta)$ is the critical angle.

Comparing the present results with the corresponding ones for electrons in gapped graphene [36], we found that the perfect interband transmission of massive pseudospin-one particles still persists in most of the cases except for the (−1,0) and (0,1) configurations. These results contrast with the complete absence of perfect interband transmission of massive pseudospin-1/2 particles [36]. Under the general focusing condition (13), the nondependence of R_{ij} on ϕ is maintained for the (−1,1), (1,−1), (1,1), and (−1,−1) systems, and its value is given by the relation $R_{ij} = (i\Delta + j\Delta')^2/V_0^2$.

One can attempt to search other SKT conditions by tuning the parameters Δ and Δ'. Nevertheless, the appearance of SKT requires that the mass terms remain the same in both regions of the step potential, Fig. 4(a). Furthermore, a small variation of energy, namely $E = V_0/2 + \delta E$, has an effect on SKT. As we show before, strong differences in the transmission as a function of ϕ are evidenced with the tuning of Δ, Δ', and

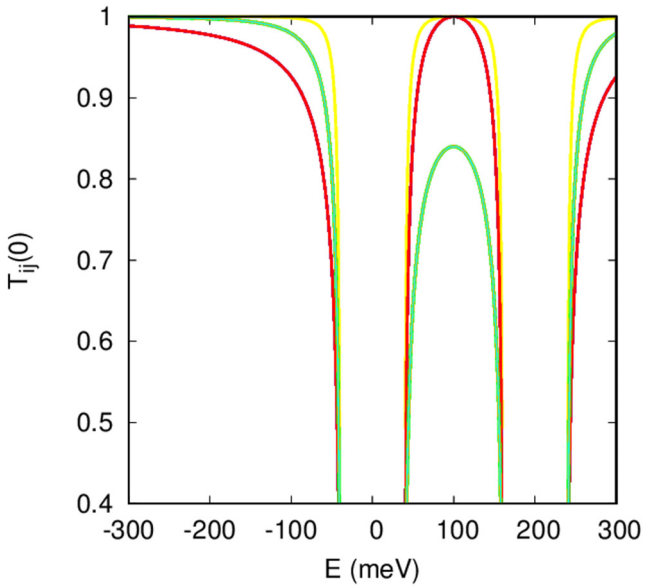

FIG. 8. Transmission probability for massive particles as a function of E for normal incidence ($\phi = 0$), for the case of pseudospin-1/2 in green, and for the case of pseudospin-one in the configurations: $(1,-1)$ and $(-1,1)$ in red and $(0,0)$ in yellow.

E for the $(0,0)$ system; see Fig. 4(a). In this way, ASKT also turns out to be susceptible to small variations of E, as shown in Fig. 4(b) for the $(1,1)$ configuration. Although small variations in a possible experimental setup could generate observable effects in the transmission for high values of ϕ, perfect and attenuated transmission are robust for a wide angular range.

In Fig. 8, we compare the transmission of massive pseudospin-one particles with the pseudospin-1/2 case, under normal incidence as a function of E. With massless particles, perfect transmission always occurs independent of the energy due to the pseudospin conservation in $\phi = 0$. However, the mass generation term changes drastically the transmission behavior within the nonrelativistic regime. The transmission probability is the same for the cases of pseudospin-1/2 and -one in the configurations $(-1,-1)$ and $(1,1)$. This indicates that the flat band location does not affect the transmission under normal incidence in these configurations. However, the flat band location modifies the transmission for other incidence angles. Thus the systems $(-1,1)$, $(0,0)$, and $(1,-1)$ responsible of the SKT are very different in the cases of pseudospin-one and 1/2.

Finally, we analyze the intriguing issue of the particle transmission from the flat band to the conduction or valence band and vice versa. Such a problem can be discussed following a similar line of thinking as for massless particles [16]. Thus the determination of reflection or transmission coefficient needs to consider the superposition of all the possible states with the same energy in regions I or II. We found that for all the limit cases involving flat bands, where the transmission of massive pseudospin-one particles is determined, a perfect reflection emerges, as shown in the Appendix. The usual perfect transmission for normal incidence in massless pseudospin-one particles involving the flat band is destroyed by the mass generation term giving rise to the perfect reflection. This effect explains the increase of the transmission probability as $|\phi|$ is increased in the interband of transmission region near to the gaps.

VI. CONCLUSIONS AND FINAL REMARKS

In summary, we have discussed the role of the flat band location in the transmission of massive pseudospin-one particles at homogeneous and heterogeneous junctions. We found that if the flat band is located in the middle of the conduction and valence band in both regions [(0,0) system], or located at the maximum valence band in region I and the minimum conduction band in region II [$(1,-1)$ system] and vice versa [$(-1,1)$ system], SKT is preserved when the mass terms are equal. In contrast, a flat band located at the minimum (maximum) of the conduction (valence) band [$(1,1)$ and $(-1,-1)$] leads to an omnidirectional transmission, which we called attenuated SKT (ASKT) and it can occur even with different masses. For those systems, the transmission under normal incidence is unaffected and matched with the transmission of massive pseudospin-1/2 particles. Furthermore, Klein tunneling is restored in the massless limit. These findings are useful to understand the role that the flat band plays in the particle transmission, as well as its effects on the optics of massive pseudospin-one particles.

ACKNOWLEDGMENTS

One of the authors (Y.B.-O.) gratefully acknowledges a scholarship from Consejo Nacional de Ciencia y Tecnología of Mexico (Conacyt-Mexico). The authors acknowledge Romeo de Coss-Martinez for a critical reading of the manuscript.

APPENDIX: TRANSMISSION OF PSEUDOSPIN-ONE PARTICLES FROM THE FLAT BAND

In this appendix, we discuss the cases involving directly the flat band: (i) $E = 0$ for $(0,j)$, (ii) $E = \pm\Delta$ for $(\pm 1,j)$, (iii) $E = V_0 \pm \Delta'$ for $(i,\pm 1)$, and (iv) $E = V_0$ for $(i,0)$.

(i) In this case, transmission probability from the flat band seems to be undetermined because the group velocity for topological states of the flat band is zero. The boundary conditions are insufficient for determining the $r(p_x)$ amplitudes which are involved in the superposition of all the topological states.

(ii) For normal incidence $\phi = 0$, wave function in region I is obtained by the superposition of a constant propagation mode and the linear combination of topological states

$$|\Psi_I\rangle = \frac{1}{2}(1+r)\begin{pmatrix}\sqrt{\alpha}\\ s\sqrt{2\gamma}\\ \sqrt{\alpha}\end{pmatrix} + \frac{1}{\sqrt{2}}\begin{pmatrix}1\\0\\-1\end{pmatrix}\int (e^{ixp/\hbar} + r_p e^{-ixp/\hbar})dp, \qquad \text{(A1)}$$

where r_p (r) is the reflection amplitude for a topological state (propagation mode) with a linear momentum p (0). In (A1), we have used the wave functions (7). In region II, the wave function has the form (10), where $\phi' = 0$ due to Snell's law (12). Equation (A1) shows that the topological states contributions do not participate in the scattering problem because ψ_2 and $\psi_1 + \psi_3$ are zero. Then, the reflection probability can be determined from (11) obtaining $R_{\pm 1j} = 1$. For $\phi \neq 0$, in the same way as in case (i), the boundary conditions are insufficient to determining all the possible r_p amplitudes.

(iii) For normal incidence, the wave function in region I is given by (9) evaluating at $\phi = 0$, whereas in region II the wave function consists of a superposition of topological states and one propagation mode,

$$|\Psi_{II}\rangle = \frac{1}{\sqrt{2}}\begin{pmatrix}1\\0\\-1\end{pmatrix}\int t_p e^{ixp/\hbar}dp + \frac{t}{2}\begin{pmatrix}\sqrt{\alpha'}\\\sqrt{2\gamma'}\\\sqrt{\alpha'}\end{pmatrix}, \qquad \text{(A2)}$$

where t_p are the parameters of the linear combination. Again, the topological states in (A2) do not contribute to the scattering problem. Hence the reflection probability is given by (11), where $R_{i\pm 1} = 1$ for $\phi = 0$ and $E = V_0 \pm \Delta'$. This result for massive pseudospin-one particles with perfect reflection at normal incidence contrasts with the massless case, where perfect transmission is always obtained [16]. For $\phi \neq 0$, the wave function in region II is written as

$$|\Psi_{II}\rangle = \frac{1}{\sqrt{2}}\int t_p \begin{pmatrix}e^{-i\phi'(p)}\\0\\-e^{i\phi'(p)}\end{pmatrix} e^{ixp/\hbar}dp. \qquad \text{(A3)}$$

Applying again the boundary conditions, the vanishing $\psi_2(x)$ component in (A3) necessarily leads to a perfect reflection because $r = 1$.

(iv) The wave function in region I is the same as (9), whereas in region II it is conformed by the linear combination of topological states

$$|\Psi_{II}\rangle = \frac{1}{\sqrt{2}}\int t_p \begin{pmatrix}\beta' e^{-i\phi'_p}\\-\sqrt{2}\frac{\Delta'}{|E-V_0|}\\-\beta' e^{i\phi'_p}\end{pmatrix} e^{ixp/\hbar}dp. \qquad \text{(A4)}$$

Since we have $\phi'_p = 0$ for normal incidence, the wave function (A4) meets the condition $\psi_1(x) + \psi_3(x) = 0$. This indicates that $r = -1$ and hence perfect reflection is again obtained. For $\phi \neq 0$, the nonzero $\psi_2(x)$ component in (A4) makes the reflection probability become undetermined.

[1] K. S. Novoselov, A. K. Geim, S. V. Morozov, D. Jiang, M. I. Katsnelson, I. V. Grigorieva, S. V. Dubonos, and A. A. Firsov, Nature (London) **438**, 197 (2005).

[2] A. H. Castro Neto, F. Guinea, N. M. R. Peres, K. S. Novoselov, and A. K. Geim, Rev. Mod. Phys. **81**, 109 (2009).

[3] T. O. Wehling, A. M. Black-Schaffer, and A. V. Balatsky, Adv. Phys. **63**, 1 (2014).

[4] O. Klein, Z. Phys. **53**, 157 (1929).

[5] M. I. Katsnelson, K. S. Novoselov, and A. K. Geim, Nat. Phys. **2**, 620 (2006).

[6] A. F. Young and P. Kim, Nat. Phys. **5**, 222 (2009).

[7] N. M. R. Peres, J. Phys.: Condens. Matter **21**, 095501 (2009).

[8] S. Borisenko, Q. Gibson, D. Evtushinsky, V. Zabolotnyy, B. Büchner, and R. J. Cava, Phys. Rev. Lett. **113**, 027603 (2014).

[9] Z. K. Liu, B. Zhou, Y. Zhang, Z. J. Wang, H. M. Weng, D. Prabhakaran, S. K. Mo, Z. X. Shen, Z. Fang, X. Dai, Z. Hussain, and Y. L. Chen, Science **343**, 864 (2014).

[10] M. Neupane, S. Y. Xu, R. Sankar, N. Alidoust, G. Bian, C. Liu, I. Belopolski, T. R. Chang, H. T. Jeng, H. Lin, A. Bansil, F. Chou, and M. Z. Hasan, Nat. Commun. **5**, 4786 (2014).

[11] M. Orlita, D. M. Basko, M. S. Zholudev, F. Teppe, W. Knap, V. I. Gavrilenko, N. N. Mikhailov, S. A. Dvoretskii, P. Neugebauer, C. Faugeras, A-L. Barra, G. Martinez, and M. Potemski, Nat. Phys. **10**, 233 (2014).

[12] F. Teppe, M. Marcinkiewicz, S. S. Krishtopenko, S. Ruffenach, C. Consejo, A. M. Kadykov, W. Desrat, D. But, W. Knap, J. Ludwig, S. Moon, D. Smirnov, M. Orlita, Z. Jiang, S. V. Morozov, V. I. Gavrilenko, N. N. Mikhailov, and S. A. Dvoretskii, Nat. Commun. **7**, 12576 (2014).

[13] B. Dóra, J. Kailasvuori, and R. Moessner, Phys. Rev. B **84**, 195422 (2011).

[14] Z. Lan, N. Goldman, A. Bermudez, W. Lu, and P. Ohberg, Phys. Rev. B **84**, 165115 (2011).

[15] D. Bercioux, D. F. Urban, H. Grabert, and W. Häusler, Phys. Rev. A **80**, 063603 (2009).

[16] D. F. Urban, D. Bercioux, M. Wimmer, and W. Häusler, Phys. Rev. B **84**, 115136 (2011).

[17] K. Essafi, L. D. C. Jaubert, and M. Udagawa, J. Phys.: Condens. Matter **29**, 315802 (2017).

[18] M. Vigh, L. Oroszlány, S. Vajna, P. San-Jose, G. Dávid, J. Cserti, and B. Dóra, Phys. Rev. B **88**, 161413 (2013).

[19] A. Fang, Z. Q. Zhang, S. G. Louie, and C. T. Chan, Phys. Rev. B **93**, 035422 (2016).

[20] R. Shen, L. B. Shao, B. Wang, and D. Y. Xing, Phys. Rev. B **81**, 041410 (2010).

[21] J. Romhanyi, K. Penc, and R. Ganesh, Nat. Commun. **6**, 6805 (2015).

[22] H. M. Price, O. Zilberberg, T. Ozawa, I. Carusotto, and N. Goldman, Phys. Rev. Lett. **115**, 195303 (2015).

[23] V. G. Veselago, Sov. Phys. Usp. **10**, 509 (1968).

[24] J. B. Pendry, Nature (London) **423**, 22 (2003).

[25] V. V. Cheianov, V. Fal'ko, and B. L. Altshuler, Science **315**, 1252 (2007).

[26] V. Apaja, M. Hyrkäs, and M. Manninen, Phys. Rev. A **82**, 041402 (2010).

[27] R. A. Vicencio, C. Cantillano, L. Morales-Inostroza, B. Real, C. Mejía-Cortés, S. Weimann, A. Szameit, and M. I. Molina, Phys. Rev. Lett. **114**, 245503 (2015).

[28] S. Mukherjee, A. Spracklen, D. Choudhury, N. Goldman, P. Öhberg, E. Andersson, and R. R. Thomson, Phys. Rev. Lett. **114**, 245504 (2015).

[29] S. Peotta and P. Törmä, Nat. Commun. **6**, 8944 (2015).

[30] A. Julku, S. Peotta, T. I. Vanhala, D. H. Kim, and P. Törmä, Phys. Rev. Lett. **117**, 045303 (2016).
[31] R. Drost, T. Ojanen, A. Harju, and P. Liljeroth, Nat. Phys. **13**, 668 (2017).
[32] M. R. Slot, T. S. Gardenier, P. H. Jacobse, G. C. P. van Miert, S. N. Kempkes, S. J. M. Zevenhuizen, C. Morais Smith, D. Vanmaekelbergh, and I. Swart, Nat. Phys. **13**, 672 (2017).
[33] L. Zhu, S. S. Wang, S. Guan, Y. Liu, T. Zhang, G. Chen, and S. A. Yang, Nano Lett. **16**, 6548 (2016).
[34] B. Trauzettel, D. V. Bulaev, D. Loss, and G. Burkard, Nat. Phys. **3**, 192 (2007).
[35] G. Cordourier-Maruri, Y. Omar, R. de Coss, and S. Bose, Phys. Rev. B **89**, 075426 (2014).
[36] M. R. Setare and D. Jahani, Physica B **405**, 1433 (2010).
[37] Y. Xu and G. Jin, Phys. Lett. A **378**, 3554 (2014).
[38] C. Xu, G. Wang, Z. H. Hang, J. Luo, C. T. Chan, and Y. Lai, Sci. Rep. **5**, 18181 (2015).
[39] V. V. Cheianov and V. I. Fal'ko, Phys. Rev. B **74**, 041403 (2006).
[40] T. Low, S. Hong, J. Appenzeller, S. Datta, and M. S. Lundstrom, IEEE Trans. Electron Devices **56**, 1292 (2009).
[41] P. E. Allain and J. N. Fuchs, Eur. Phys. J. B **83**, 301 (2011).
[42] C. W. J. Beenakker, Rev. Mod. Phys. **80**, 1337 (2008).